THE EFFECTS OF DIAPHRAGM FLEXIBILITY ON THE SEISMIC PERFORMANCE OF LIGHT FRAME WOOD STRUCTURES

R. Pathak[1] and F. A. Charney[2]

[1] *FEA Specialist, Bentley Systems Inc., Carlsbad, California, USA*

[2] *Associate Professor, Civil Engineering Department, Virginia Tech, Blacksburg, Virginia, USA*

Email: Rakesh.Pathak@bentley.com

ABSTRACT:

Several experimental and mathematical studies on light frame wood structures (LFWS) have been performed in the last few decades. The current residential design guideline still does not consider the actual flexibility of diaphragm in analyzing LFWS when they are subjected to lateral loads. For lateral force distribution, the guideline assumes the in-plane stiffness of diaphragm as either negligible or infinite. This paper presents work targeted to study the effects of diaphragm flexibility on the seismic performance of LFWS. Finite element models of various LFWS are created and nonlinear response history analyses are performed using the Imperial Valley and Northridge ground motions. These analyses encompass the parametric study on the LFWS with varying aspect ratios, diaphragm flexibility and lateral force resisting system. Torsionally irregular house models showed the largest range of variation in peak base shear of individual shear walls, when corresponding flexible and rigid diaphragm models are compared. It is found that presence of an interior shear wall helps in reducing peak base shears in the boundary walls of torsionally irregular models. The presence of interior wall was also found to reduce the flexibility of diaphragm. A few analyses also showed that the nail connections are the major source of in-plane flexibility compared to sheathings within a diaphragm, irrespective of the aspect ratio of the diaphragm.

KEYWORDS: Diaphragm Flexibility, Nonlinear, Response History Analysis, Finite Element

1. INTRODUCTION

Practicing structural engineers rely heavily on the structural behavior observed in experiments or the results obtained from validated analytical models. In the case of LFWS, neither can be economically performed and thus in practice this has resulted in the development of simplified procedures to obtain the force distribution in the structural members. These procedures are only applicable to simple structures, and for complex structures good engineering judgment is required. The residential structural design guide (NAHBRC 2000) document specifies that: "*Designer judgment is essential in the early stages of design because the analytic methods and assumptions used to evaluate the lateral resistance of light-frame buildings are not in themselves correct representations of the problem. They are analogies that are sometimes reasonable but at other times depart significantly from reason and actual system testing or field experience*".

The design of wood structures follows one of the three popular approaches: (a) tributary area, (b) total shear and (c) relative stiffness. The tributary area approach considers the diaphragm as completely flexible and assigns forces to the shear walls based on the proportion of the area of the diaphragm it covers. The total shear approach uses the story shear to calculate the total wall length required to resist the force in each direction of loading and then distributes the obtained wall length on that story based on the engineer's view. The relative stiffness method assumes the horizontal diaphragm as rigid compared to the shear walls. This results in a force distribution based on the relative stiffnesses of the shear walls. It is interesting to note that these three approaches may give significantly different forces in the shear walls for the same structural design. The tributary area and relative stiffness are the most practiced approaches used in distributing the lateral forces to various shear walls in LFWS design. In reality,

none of the approaches may be accurate, as the actual diaphragm stiffness will most likely lie somewhere between entirely flexible and entirely rigid. Thus, an approach which considers the response of LFWS based on actual modeling of the structural elements in the diaphragm is most appropriate.

This paper investigates the effect of diaphragm flexibility on the seismic response of LFWS and compares it with in-plane rigid diaphragm model response. To accomplish this, finite element models of various LFWS have been developed and nonlinear response history analyses are performed. These models are in general based on the work done by Kasal et al. (1994) and Collins et al. (2005). However, no substructuring or submodeling of subassemblages is performed, and instead a detailed model considering almost every connection in the shear walls and diaphragms is developed. The studs, plates, sills, blockings and joists are modeled using linear isotropic 3D frame elements. A linear orthotropic shell element incorporating both membrane and plate behavior is used for the sheathings. The connections are modeled using nllinks having oriented spring pair (Judd and Fonseca 2005) with modified Stewart hysteresis spring stiffnesses. The oriented spring pair has been found to give a more accurate representation of the sheathing to framing connections in shear walls and diaphragms when compared to non-oriented or single springs typically used by other researchers. The modified Stewart hysteresis model is chosen because of its computational efficiency, as it is based on mostly linear path following rules and accurately represents the connections' pinching behavior with strength, stiffness degradation and removal (Folz and Filiatrault 2001). It is also one of the latest state of the art model used in representing dowel type connector stiffness in LFWS. The details of the modeling methodology used in developing finite element models presented in this study are discussed in Pathak (2008).

2. LFWS MODELS DESCRIPTION

The LFWS selected for modeling and analysis are classified into seven different types based on their geometry. Each type contains up to 4 models with different shear wall configuration. The roof plans for type 1 models is shown in Figure 1. The corresponding finite element models as viewed in SAP2000 (CSI 2000) GUI are shown in Figure 2. The models 1 and 2 in each type creates a symmetric lateral force resisting system along both X and Y global directions. The models 3 and 4 in each type have one and two walls missing, respectively, compared to model 1 and this results in an asymmetric lateral force resisting system. The aspect ratio of the house plan in these models varies from 1 to 5 and is kept constant within the same type of models. Two aspect ratios are defined for each type and are referred to as X and Y direction aspect ratio. The X direction aspect ratio is calculated as the ratio of the Y dimension to the X dimension of the floor plan in a model. Similarly, the Y direction aspect ratio is calculated as the ratio of the X dimension to the Y dimension of the floor plan in a model. These ratios are defined because in a few models the earthquake loading is applied in both X and Y directions simultaneously and some of these models have different lateral force resisting systems along the X and Y directions. These direction aspect ratios will be used to correlate with the direction response later in the discussion. Table 1 presents the direction aspect ratios and the periods of vibration in the two translational modes and one rotational mode about the vertical Z-axis of the entire flexible and rigid diaphragm house model 1 used in the analysis. These periods of vibration are calculated using the initial stiffness of the elements in the structure, and they change over the course of loading because of the yielding occurring in the connection elements.

The material, nails, sheathing and frame properties are kept constant in all the models except where model diaphragm flexibility is modified. In all the models the shear walls are 8' x 8' with studs spaced at 2' intervals, and have two 4' x 8' OSB panels. The area between the shear walls on the boundary is covered by stud framing spaced at 2' intervals. All the walls have a double top plate and a mid-height blocking which also extends on the boundary between the shear walls. In the models where the shear wall is removed from the boundary, only the sheathing panels and their connecting nails are removed and not the stud framing, as can be seen in Figure 2. The roof diaphragm consists of 4' x 8' and 8' x 8' OSB sheathing panels, joists, blockings and nails. In all the models, the same nails are used in connecting the sheathing to framing and framing to framing. The frame and panel self-mass is calculated using the mass per unit volume of the wood by using the assumed specific gravity of 0.55. This

specific gravity results in a mass per unit volume of 5.144 x 10^{-8} kips-sec^2/in^4. The nail mass is neglected in all the models, and in all the models a mass of 0.06 kips-sec^2/in. is applied, which is uniformly distributed on the roof nodes.

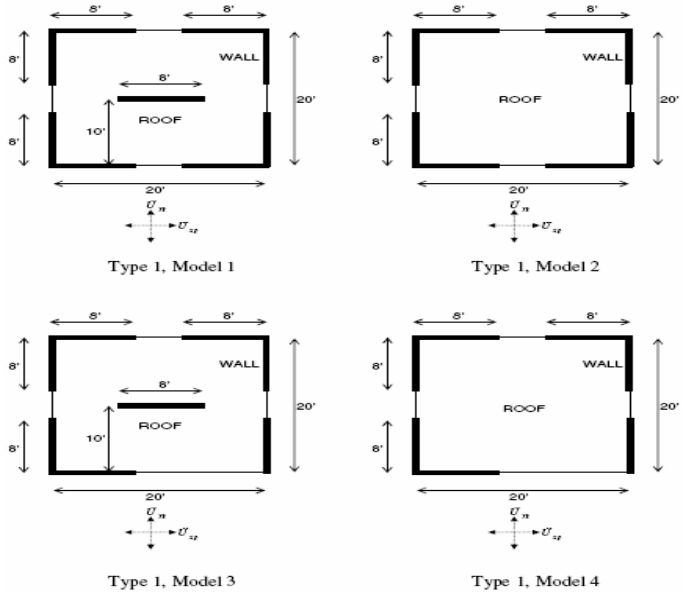

Figure 1: Type 1 floor plans

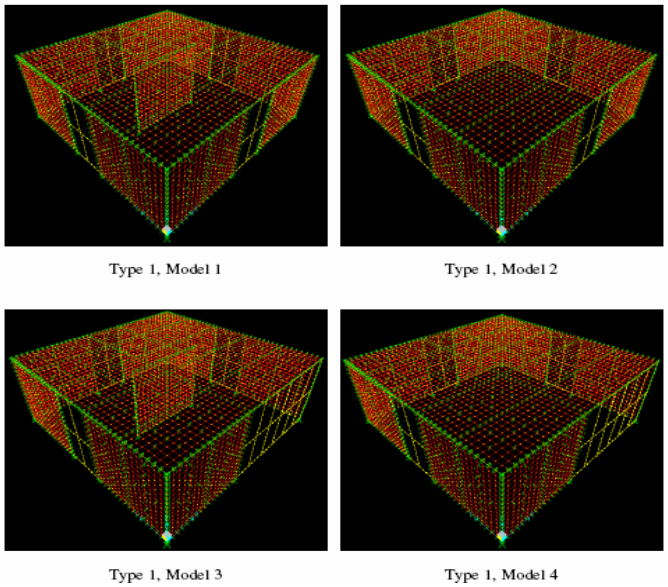

Figure 2: Type 1 finite element house models

Table 1: Direction aspect ratios and vibration periods of model 1 in all the types

	DIRECTION ASPECT RATIO		FLEXIBLE DIAPHRAGM VIBRATION PERIODS (sec)			RIGID DIAPHRAGM VIBRATION PERIODS (sec)		
MODEL 1	X	Y	X	Y	θ	X	Y	θ
TYPE 1	1.00	1.00	0.279	0.322	0.187	0.243	0.271	0.167
TYPE 2	0.50	2.00	0.270	0.454	0.242	0.247	0.385	0.215
TYPE 3	0.33	3.00	0.271	0.499	0.267	0.245	0.382	0.221
TYPE 4	0.20	5.00	0.265	0.559	0.289	0.242	0.379	0.226
TYPE 5	1.00	1.00	0.349	0.334	0.219	0.334	0.291	0.204
TYPE 6	2.00	0.50	0.353	0.305	0.242	0.333	0.288	0.225
TYPE 7	5.00	0.20	0.383	0.288	0.281	0.335	0.281	0.240

All the 7 house types have a total of 22 models with flexible diaphragms. These flexible diaphragm models in-plane member properties are modified to get 22 corresponding in-plane rigid diaphragm models. In addition to these 44 models, two sets of model 2 from types 2, 3, and 4 and two sets of model 1 from types 5, 6 and 7 are created with the following diaphragm flexibility: (a) sheathings are modeled as rigid in-plane with nails and joists as flexible, and (b) nail connections are modeled as rigid in-plane and sheathing and joist as flexible. These models are used to coarsely uncouple and measure the relative contribution of flexibility sources in the diaphragm response.

3. NONLINEAR RESPONSE HISTORY ANALYSIS

All the 56 resulting house models are subjected to the first twelve seconds of either Imperial Valley or Northridge earthquake records or both, scaled to 0.30g and 0.10g in X and Y directions respectively. The necessity of nonlinear analysis arises from the nonlinear nature of the various connections occurring in the LFWS systems. Also, as the

structure is subjected to an earthquake, it tends to yield and degrade in strength and stiffness over the course of loading. All the models presented in this study are analyzed using a new high performance finite element analysis program developed by the authors (Pathak 2008). To perform nonlinear response history analysis, the program formulates the equation of motion as shown in equation (1) and uses Newmark's constant average acceleration method for direct numerical integration over the time domain. The full Newton-Raphson iteration method with an energy based convergence criteria (Chopra 2001) is used within a time step to reduce the error introduced by the use of the tangent stiffness matrix instead of the unknown secant stiffness matrix. The time step chosen for the dynamic analysis of all the models is 0.005 seconds which is one-fourth of the input loading time interval. A convergence study using a refined time steps of 0.00125 and 0.000625 seconds was performed on a few selected models prior to all the analysis.

$$[M](\ddot{U})+[C](\dot{U})+[K](U)=-[M][i](\ddot{U}_g) \tag{1}$$

3.1 Mass Matrix

The mass matrix [M] in equation (1) is assembled by adding the mass contribution of elements and nodes to each translational degree of freedom. This is a lumped mass matrix and hence is diagonal. The mass contribution in the house models comes from the self-weight of frames, sheathings and the superimposed nodal mass representing other loads on the horizontal diaphragm. The mass contribution from the nails is neglected in all the models.

3.2 Damping Matrix

The damping matrix [C] in equation (1) is linear and is based on the equivalent viscous damping mechanism distributed throughout the structure. This matrix for all the finite element models is considered as mass proportional and is shown in equation (2). Experiments on light frame wood structural systems have shown that at large displacement amplitudes, the fasteners and other connections are the predominant sources of hysteretic damping and non-viscous energy dissipation. These characteristics of fasteners and connections are already included in their force-deformation relationships. The hysteretic damping effect which comes into play at large displacement amplitude also justifies the use of mass proportional damping which provides lesser damping in higher frequency modes. In these analyses it is assumed that no errors get introduced due to low damping in higher modes. Also, there was no visible error in the responses obtained for any of the models, which could be attributed to low damping in higher modes. To incorporate the equivalent viscous damping in LFWS model, the damping constant (α_0) in equation (2) is assigned a value based on the damping ratio, which is 2% of the critical at the X translational frequency of vibration. The damping ratio in the range of 1% to 5% has been found suitable for most wood structural systems (Chui and Smith 1989, Yeh et al. 1971).

$$[C]=\alpha_0[M] \tag{2}$$

3.3 Global Stiffness Matrix

The global stiffness matrix [K] in equation (1) is nonlinear and is formulated by assembling the global stiffness matrix of all the individual elements in the model. This matrix can be seen as a sum of linear and nonlinear element matrices as shown in equation (3). The numerical values in K_L are the contributions from linear frames and shells and remain constant throughout the analysis. The numerical values in K_N come from nllinks representing fasteners and intercomponent connections in the models, and they change with the internal deformations within the elements.

$$[K]=[K_L]+[K_N] \quad (3)$$

3.4 Loading

The right hand side of equation (1) represents the dynamic loading vector which is the product of mass matrix, influence coefficient matrix [*i*] and the ground motion history used in the respective analysis.

4. RESULTS

4.1 Flexible and Rigid Diaphragm Response Comparison

It is found that the flexible and rigid diaphragm assumptions give different in-plane peak base shears in corresponding walls of all the models. The rigid diaphragm assumption overestimates and underestimates in-plane peak base shear in the walls when compared with the results from corresponding models of flexible diaphragm. The rigid diaphragm assumption overestimated and underestimated the in-plane peak base shears of maximum up to 28% and 33%, respectively. These maximum values were obtained for torsionally irregular models, and for the symmetric lateral load resisting system with interior wall analyzed herein, this range comes down to 9% (underestimation) and 16% (overestimation). Tables 3 and 4 present the ratios of peak in-plane base shears obtained using rigid and flexible diaphragm assumptions for various walls in types 1 and 4 models using Imperial Valley earthquake loading.

Table 3: Type 1 models

	RIGID/FLEXIBLE			
	PEAK IN-PLANE BASE SHEAR RATIO			
WALL #	TYP1M1	TYP1M2	TYP1M3	TYP1M4
1	1.16	1.09	1.02	0.98
2	1.16	1.09	x	x
3	1.16	1.09	1.15	1.07
4	1.16	1.09	1.15	1.07
5	**0.95**	x	0.96	x
6	1.05	1.02	1.10	1.19
7	1.05	1.02	1.10	1.19
8	1.05	1.02	**1.28**	1.24
9	1.05	1.02	**1.28**	1.24

Table 4: Type 4 models

	RIGID/FLEXIBLE			
	PEAK IN-PLANE BASE SHEAR RATIO			
WALL #	TYP4M1	TYP4M2	TYP4M3	TYP4M4
1	0.97	**1.05**	1.03	1.00
2	0.97	**1.05**	x	x
3	0.97	**1.05**	1.02	0.98
4	0.97	**1.05**	1.01	0.98
5	0.92	x	1.03	x
6	0.81	0.76	**0.74**	0.76
7	0.81	0.76	1.03	0.93

- x indicates wall is not present in the model
- numbers in bold present maximum and minimum ratio

4.2 Peak In-Plane Base Shear in Partition Walls

The ratio of peak in-plane base shear per unit length in the interior shear wall and the peak in-plane base shear per unit length in the outer shear walls is calculated for all the flexible and rigid diaphragm cases of symmetric models. The idea is to compare the relative variation in interior wall forces when the direction aspect ratio and the flexibility of the model changes. Figures 3 and 4 present these results for flexible and rigid diaphragm cases, respectively, for the two different lateral force resisting systems combined in one plot. In the flexible diaphragm models, as the X direction aspect ratio increases, an increase in interior wall peak base shear per unit length relative to the outer walls peak base shear per unit length is suggested from Figure 3. Figure 4 suggests just the opposite trend for the rigid diaphragm models.

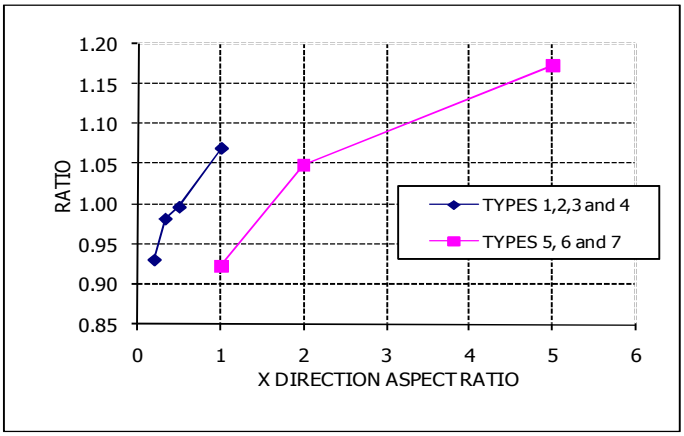

Figure 3: Ratio of interior and exterior shear wall in-plane peak base shear per unit length Vs the X direction aspect ratio, flexible diaphragm model 1

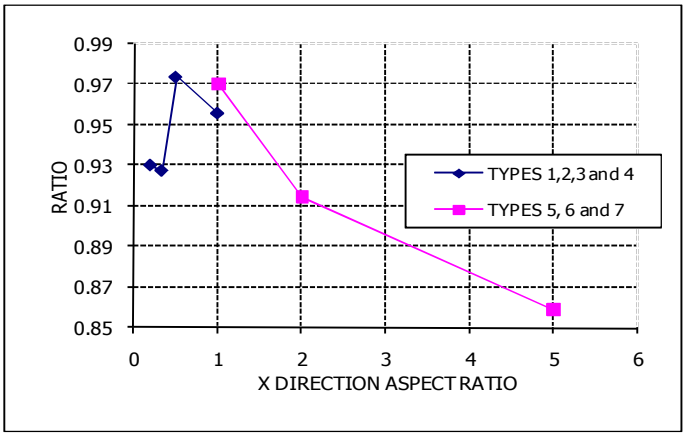

Figure 4: Ratio of interior and exterior shear wall in-plane peak base shear per unit length Vs the X direction aspect ratio, rigid diaphragm model 1

4.3 Effects of Torsional Irregularity

Torsional irregularity refers to the change in the stiffness center relative to the center of mass in the structure. So, when loading is applied to such irregular systems, it induces torsional moments in the system. This moment is shared by all the walls, resulting in a change of their base shears, the sign and magnitude of which vary from wall to wall in a model. It is found that there were significant changes in in-plane peak shear forces occurring in the walls due to the introduction of torsional irregularity using both the flexible and rigid diaphragm modeling assumption. However, these changes were significantly different for some cases using these two assumptions.

4.4 Study using the Code Specified Measure of Rigidity

The design code specifies that the horizontal diaphragms can be considered to be rigid until the maximum floor deflection exceeds twice the wall displacement. We apply this criterion along X and Y directions for symmetric models and denote it generically as RC_d, where RC denotes rigidity criteria and the subscript d is the direction in which it is measured. This criterion in a direction d is linked with the direction aspect ratio and is generically referred to as AR_d.

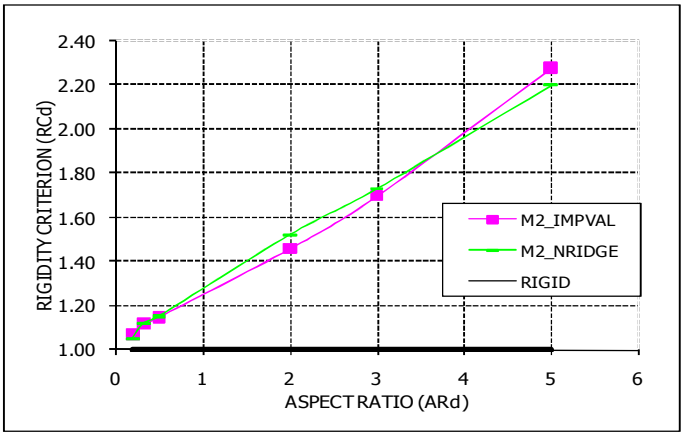

Figure 5: Rigidity criterion plot for types 2, 3 and 4 model 2

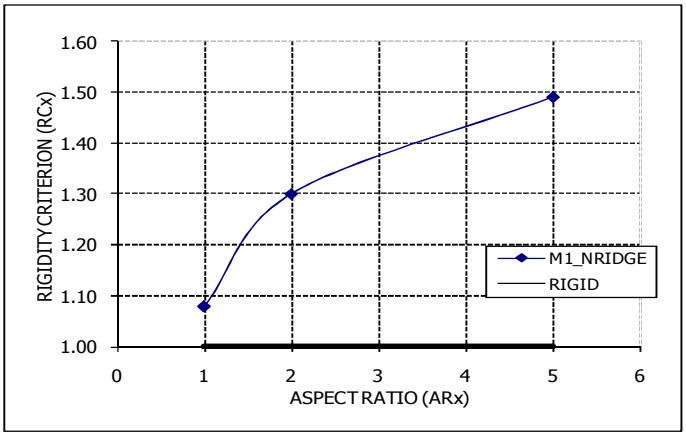

Figure 6: Rigidity criterion plot for types 5, 6 and 7 model 1

Figure 5 present the rigidity criterion plot for symmetric model 2 which has no interior shear wall and we note that as the aspect ratio increases the flexibility of diaphragm increases. Figure 6 on the other hand present the rigidity criterion plot for symmetric models having an interior shear wall. The comparison of these two plots shows that diaphragm flexibility is reduced for the model having interior shear wall in them.

The diaphragm constitutes joists, sheathing and nail connections, which are the sources of flexibility in its response. These flexibility sources were coarsely uncoupled to measure the relative contribution of nails and sheathings for types 2, 3 and 4 model 2 and types 5, 6 and 7 model 1. The rigidity criterion is plotted for these two sets in the Figures 7 and 8 respectively. It is found that nail connections are the major source of flexibility compared to sheathings in the diaphragm throughout the range of aspect ratio studied. This behavior is consistent for the models with or without interior wall.

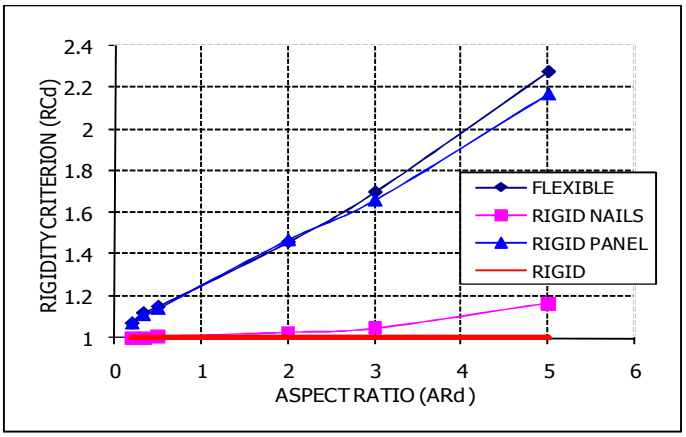

Figure 7: Rigidity criterion plot for types 2, 3 and 4 model 2 with various in-plane diaphragm flexibilities

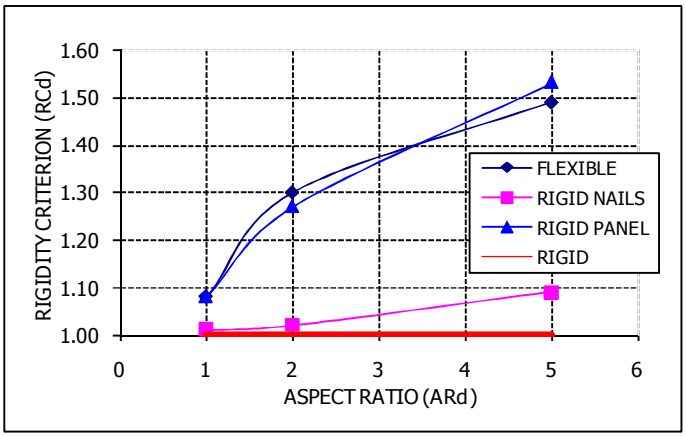

Figure 8: Rigidity criterion plot for types 5, 6 and 7 model 1 with various in-plane diaphragm flexibilities

5. SUMMARY, CONCLUSIONS AND RECOMMENDATIONS

A parametric study is performed to understand the diaphragm flexibility on the seismic response of light frame wood structures. Various light frame house models with different plan and shear wall configuration have been analyzed. The analysis of torsionally irregular flexible and rigid diaphragm systems showed greatest difference in their response. Thus, incorporating flexibility of diaphragm in torsionally irregular systems shall certainly minimize significant errors. The interior shear walls resist a significant amount of seismic forces in their planes and the distribution depends upon the aspect ratio of the diaphragm, its flexibility and the stiffness of the shear walls. In the above analysis the stiffnesses of all the walls are kept the same, and hence only the variation of shear force in the interior shear wall with changing aspect ratio and flexibility is captured. It is found that in the symmetric flexible diaphragm models, as the aspect ratio increases, an increase in interior wall peak base shear per unit length relative to the outer walls peak base shear per unit length is suggested. This ratio of peak base shears is approximately 1.18 for the diaphragm aspect ratio of 5 showing response more close to infinitely rigid diaphragm behavior than entirely flexible diaphragm behavior. Stiffness irregularity increases the yielding and energy dissipation in some walls and hence identifying such walls in a structural system is critical from design perspective. The in-plane flexibility of a diaphragm is found to get significantly affected by the presence of interior shear wall located at the geometric center in the direction of loading. This effect due to an interior wall shall vary depending upon the spatial location and needs further investigation. The nail connections are the major source of in-plane flexibility compared to sheathings within a diaphragm, irrespective of the aspect ratio of the diaphragm. This estimate however is established using a very coarse uncoupling procedure applicable only to linear systems. New procedures need to be devised to uncouple individual element response accurately in nonlinear response history analysis of LFWS.

REFERENCES:

NAHBRC (2000). *Residential Structural Design Guide: 2000 Edition,* U.S. Department of Housing and Urban Development, Rockville, MD, USA.

Collins, M., Kasal, B., Paevere, P., and Foliente, G. C. (2005). Three Dimensional Model of Light-Frame Wood Buildings I: Model Description. *Journal of Structural Engineering*, **131:4**, 676-683.

Chopra, A. (2001). Dynamics of Structures, Prentice Hall of India Private Limited, New Delhi, India.

Chui, Y. H., and Smith, I. (1989). Quantifying Damping in Structural Timber Components. Proc., 2nd Pacific Timber Engineering Conference., Institute of Professional Engineers., Wellington, NZ, **1**, 57-60.

CSI. (2000). SAP2000: Integrated Software for Structural Analysis and Design. Computers and Structures, Inc., Berkeley.

Folz, B., and Filiatrault, A. (2001). Cyclic Analysis of Wood Shear Walls. *Journal of Structural Engineering*, **127:4**, 433-441.

Judd, J. P., and Fonseca, F. S. (2005). Analytical Model for Sheathing-to-Framing Connections in Wood Shear Walls and Diaphragms. *Journal of Structural Engineering*, **131:2**, 345-352.

Kasal, B., Leichti, R. J., and Itani, R. Y. (1994). Nonlinear Finite-Element Model of Complete Light-Frame Wood Structures. *Journal of Structural Engineering*, **120:1**, 100-119.

Pathak, R. (2008). The Effects of Diaphragm Flexibility on the Seismic Performance of Light Frame Wood Structures, PhD Dissertation, Virginia Polytechnic Institute and State University, Blacksburg, VA, USA.

Yeh, T. C., Hartz, B. J., and Brown, C. B. (1971). Damping Sources in Wood Structures. *Journal of Sound and Vibration*, **19:4**, 411-419.